Supplementary Material

TABLE I: Variables used in the random forest classifiers, given in categories of object kinematics, angular variables, and event kinematics. The symbol (†) denotes a measurement in the rest frame of the reconstructed H boson. A subset of these is used for each channel and data-taking period.

Object Kinematics	
Lepton energy	E^ℓ
Lepton/jet transverse momentum	$p_T^\ell, p_T^{j_1}, p_T^{j_2}$
Angular Variables	
Azimuthal angles	$\Delta\phi(j_1, j_2), \Delta\phi(\ell, \not{E}_T)$,
	$\min[\Delta\phi(\not{E}_T, j_1), \Delta\phi(\not{E}_T, j_2)], \min[\Delta\phi(\ell, j_1), \Delta\phi(\ell, j_2)]$
	$\Delta\phi(\text{bisector of dijet pair}, \not{E}_T)$
Polar angles	$\Delta\eta(j_1, j_2)$
$\eta - \phi$ combinations	$\Delta R(j_1, j_2), \max[\Delta R(\ell, j_1), \Delta R(\ell, j_2)], \min[\Delta R(\not{E}_T, j_1), \Delta R(\not{E}_T, j_2)]$
3D angles	$\text{angle}(j_1, j_2)^\dagger, \text{angle}(j_1, \text{reconstructed } W \to \ell\nu)^\dagger, \text{angle}(\ell, \text{dijet system})$
Event Kinematics	
Velocity	$\beta(\text{dijet system})$
Transverse momentum sums	$\not{E}_T, p_T(\text{dijet system}), p_T(\text{leptonic } W)$
	$H_T(j_1, j_2)$, $H_T(\text{all jets})$, $H_T(j_1, j_2, \ell)$, $H_T(j_1, j_2, \ell, \not{E}_T)$
Topological variables[a]	$\text{aplanarity}(j_1, j_2, \ell, \nu)$
	$\text{centrality}(\ell, j_1, j_2)$, $\text{centrality}(\ell, \text{all jets})$
	$\text{sphericity}(\ell, j_1, j_2)$, $\text{sphericity}(\ell, j_1, j_2, \not{E}_T)$
"N"-body masses	dijet mass : $M(j_1, j_2)$, $M(j_1, j_2, \ell)$, $M(WW)$, WW "visible mass": $M(j_1, j_2, \ell, \not{E}_T)$
Transverse masses	$M_T(j_1, j_2)$, $M_T(W \to \ell\nu)$, $M_T(WW)$
Ratio of jet energies	$E^{j_2}/E^{j_1\,\dagger}$
$KT^{\max/\min}$	$\Delta R(j_1, j_2) \cdot E_T(j_{1/2})/(E_T^\ell + \not{E}_T)$
Other combinations	scalar product of $\not{E}_T$ and angular bisector of dijet pair
	$\Delta\phi(W^\ell, \text{bisector of dijet system})$
	Magnitude of $p_T{}^{j_1}$ perpendicular to dijet system
Scaled $\not{E}_T$	$\sum_{\text{all jets}} [\sqrt{E^{j_i}} \sin(\theta^{j_i}) \cos(\Delta\phi(j_i, \not{E}_T))]^2$

[a] For descriptions of the topological variables see: V.D. Barger and R.J.N. Phillips, Collider Physics, Addison-Wesley, Reading, MA, 1987.

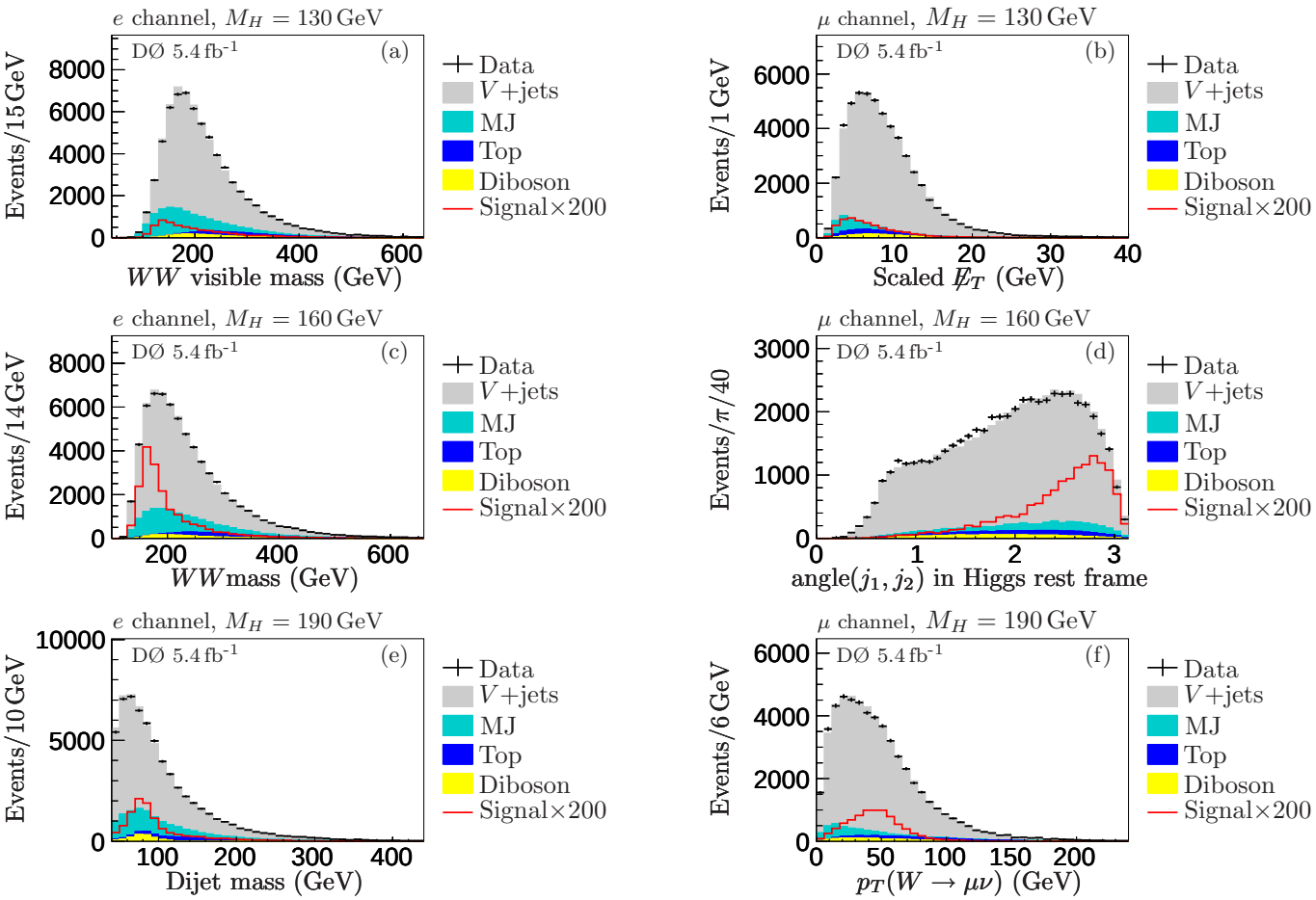

FIG. 1: Sample of DT inputs for (a,c,e) electron and (b,d,f) muon channels. The data are shown as points with uncertainties. The background contributions are shown as histograms, with sources indicated in the legend. "V+jets" includes (W/Z)+(u, d, s, c, b, g) jets, MJ is the multijet background, "top" includes pair and single top quark production, diboson includes WW, WZ, and ZZ processes. The distributions for signal are multiplied by a factor of 200.

TABLE II: Systematic uncertainties for the electron and muon channels. Signal uncertainties are shown for $M_H = 160\,\mathrm{GeV}$ for all channels except for WH, shown for $M_H = 115\,\mathrm{GeV}$. Those affecting the shape of the RF discriminant are indicated with "Y." Uncertainties are listed as relative changes in normalization, in percent, except for those also marked by "S," where the the overall normalization is constant, and the value given denotes the maximum percentage change from nominal in any region of the distribution.

Contribution	Shape	W+jets	Z+jets	top	diboson	$gg \to H$	$qq \to qqH$	WH
Jet energy scale	Y	$\left(^{+6.7}_{-5.4}\right)^S$	< 0.1	± 0.7	± 3.3	$\left(^{+5.7}_{-4.0}\right)$	± 1.5	$\left(^{+2.7}_{-2.3}\right)$
Jet identification	Y	$\pm 6.6^S$	< 0.1	± 0.5	± 3.8	± 1.0	± 1.1	± 1.0
Jet resolution	Y	$\left(^{+6.6}_{-4.1}\right)^S$	< 0.1	± 0.5	$\left(^{+1.0}_{-0.5}\right)$	$\left(^{+3.0}_{-0.5}\right)$	± 0.8	± 1.0
Association of jets with PV	Y	$\pm 3.2^S$	$\pm 1.3^S$	± 1.2	± 3.2	± 2.9	± 2.4	$\left(^{+0.9}_{-0.2}\right)$
Luminosity	N	n/a	n/a	± 6.1	± 6.1	± 6.1	± 6.1	± 6.1
Muon trigger	Y	$\pm 0.4^S$	< 0.1	< 0.1	< 0.1	< 0.1	< 0.1	< 0.1
Electron identification	N	± 4.0	± 4.0	± 4.0	± 4.0	± 4.0	± 4.0	± 4.0
Muon identification	N	± 4.0	± 4.0	± 4.0	± 4.0	± 4.0	± 4.0	± 4.0
ALPGEN tuning	Y	$\pm 1.1^S$	$\pm 0.3^S$	n/a	n/a	n/a	n/a	n/a
Cross Section	N	± 6	± 6	± 10	± 7	± 10	± 10	± 6
Heavy-flavor fraction	Y	± 20	± 20	n/a	n/a	n/a	n/a	n/a
PDF	Y	$\pm 2.0^S$	$\pm 0.7^S$	$< 0.1^S$	$< 0.1^S$	$< 0.1^S$	$< 0.1^S$	$< 0.1^S$
			Electron channel			Muon channel		
Multijet Background	Y		± 6.5			± 26		

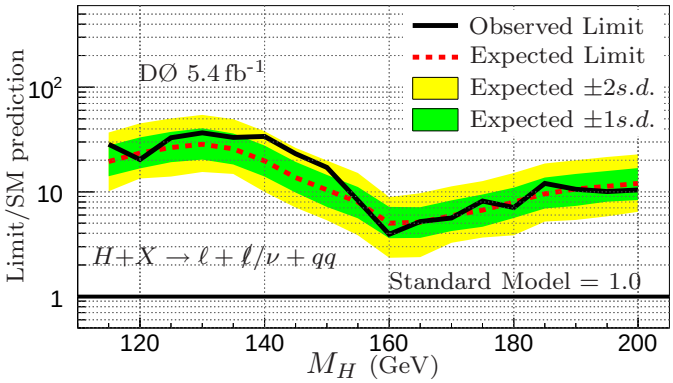

FIG. 2: Ratio of the 95% CL limit to the SM expectation as a function of M_H for the electron and muon channels combined. Expected limits are shown by the dashed line, observed limits are shown by the solid line. The heavy and light shaded areas correspond to one and two standard deviations (s.d.) around the expected result for the background-only hypothesis.